Well funneled nuclear structure landscape: renormalization

A. Idini [1],* G. Potel[2],† F. Barranco [3],‡ E. Vigezzi [4],§ and R.A. Broglia [5,6]¶

[1] *Department of Physics, University of Jyvaskyla, FI-40014 Jyvaskyla, Finland*

[2] *Lawrence Livermore National Laboratory, USA*

[3] *Departamento de Física Aplicada III,*

Escuela Superior de Ingenieros, Universidad de Sevilla,

Camino de los Descubrimientos, Sevilla, Spain

[4] *INFN Sezione di Milano, Via Celoria 16, I-20133 Milano, Italy*

[5] *Dipartimento di Fisica, Università di Milano,*

Via Celoria 16, I-20133 Milano, Italy and

[6] *The Niels Bohr Institute, University of Copenhagen, DK-2100 Copenhagen, Denmark*

(Dated: April 30, 2015)

Abstract

A complete characterization of the structure of nuclei can be obtained by combining information arising from inelastic scattering, Coulomb excitation and $\gamma-$decay, together with one- and two-particle transfer reactions. In this way it is possible to probe the single-particle and collective components of the nuclear many-body wavefunction resulting from their mutual coupling and diagonalising the low-energy Hamiltonian. We address the question of how accurately such a description can account for experimental observations. It is concluded that renormalizing empirically and on equal footing bare single-particle and collective motion in terms of self-energy (mass) and vertex corrections (screening), as well as particle-hole and pairing interactions through particle-vibration coupling allows theory to provide an overall, quantitative account of the data.

* andrea.idini@gmail.com

† gregory.potel@gmail.com

‡ barranco@us.es

§ vigezzi@mi.infn.it

¶ broglia@mi.infn.it

Nuclear structure is both a mature [1–3] and a very active field of research [4, 5] , and time seems ripe to attempt a balance of our present, quantitative understanding of it. Here we take up an aspect of this challenge and try to answer to the question: how accurately can theory predict structure observables in terms of single-particle and collective degrees of freedom and of their couplings?

In pursuing this quest one of two paths can be taken: 1) select one nuclear property, for example the single-particle spectrum, and study it throughout the mass table [6]; 2) select a target nucleus A which has been fully characterized through inelastic scattering and Coulomb excitation ($A(\alpha,\alpha')A^*$), together with one- ($A(d,p)A+1, A(p,d)A-1$) and two- (($A+2(p,t)A, A(p,t)A-2$) particle transfer processes and study the associated, complete nuclear structure information involving the island of nuclei A, $A\pm1$ and $A\pm2$ in terms of the corresponding absolute differential cross sections and decay transition probabilities. Here we have chosen the second way and selected the group of nuclei ^{118,119,120,121,122}Sn involved in the characterization of the spherical, superfluid ^{120}Sn target nucleus.

Single-particle and collective vibrations constitute the basis states. The calculations are implemented in terms of a SLy4 effective interaction and a $v_{14}(^1S_0)(\equiv v_p^{bare})$ Argonne pairing potential. HFB provides an embodiment of the quasiparticle spectrum while QRPA a realization of density ($J^\pi = 2^+, 3^-, 4^+, 5^-$) and spin ($2^\pm, 3^\pm, 4^\pm, 5^\pm$) modes. Taking into account renormalisation processes (self-energy, vertex corrections, phonon renormalization and phonon exchange) in terms of the particle-vibration coupling (PVC) mechanism, the dressed particles as well as the induced pairing interaction v_p^{ind} were calculated (see [7]; see also [8–15]). Adding v_p^{ind} to the bare interaction v_p^{bare}, the total pairing interaction v_p^{eff} was determined. With these elements, the Nambu-Gor'kov (NG) equation was solved selfconsistently using Green's function techniques [16–20], and the parameters characterizing the renormalized quasiparticle states obtained. Within this framework, the quasiparticle energies $\tilde{E}_\nu$ are given by $\tilde{E}_\nu = \sqrt{(\tilde{\epsilon}_\nu - \epsilon_F)^2 + \tilde{\Delta}_\nu^2}$. The renormalised single-particle energy $\tilde{\epsilon}_\nu - \epsilon_F = Z_\nu[(\epsilon_\nu - \epsilon_F) + \Sigma_\nu^{even}]$, is written in terms of the HF energy ϵ_ν and of the even part of the normal self-energy, the quantity Z_ν providing a measure of the single-particle character of the orbital ν. The state dependent pairing gap $\tilde{\Delta}_\nu = \tilde{\Delta}_\nu^{bare} + \tilde{\Delta}_\nu^{ind}$ obeys the generalized gap equation

$$\tilde{\Delta}_\nu = -Z_\nu \sum_{\nu'>0} \langle \nu'\bar{\nu}'|v_p^{bare} + v_p^{ind}|\nu\bar{\nu}\rangle N_{\nu'} \frac{\tilde{\Delta}_{\nu'}}{2\tilde{E}_{\nu'}}, \tag{1}$$

where $N_\nu = \tilde{u}_\nu^2 + \tilde{v}_\nu^2$ and $Z_\nu = \left(1 - \frac{\Sigma_\nu^{odd}}{\tilde{E}_\nu}\right)^{-1} = m/(m_\omega)_\nu$, Σ_ν^{odd} being the odd part of the normal self-energy, while m_ω is the $\omega-$mass. The resulting values of $\tilde{\Delta}_\nu$ are shown in Fig.1. The contribution of v_p^{bare} and v^{ind} to $\tilde{\Delta}_\nu$ are about equal, density modes leading to attractive contributions which are partially cancelled out by spin modes, as expected from general transformation properties of the associated operators entering the particle-vibration coupling vertices [21–23]. Theory (SLY4 +QRPA+ (PVC) REN+NG) provides a quantitative account of the experimental value ($\Delta^{exp} \approx 1.45$ MeV). It is to be noted that in carrying out the above calculations use has been made of empirically renormalized collective modes. This is because SLy4 leads to little collective density vibrations (cf. Table 1, where, for concreteness, the bare QRPA results characterizing the low-lying 2^+ of ^{120}Sn are collected [7], see also [24]), in keeping with the associated value of the effective mass 0.7 m. In fact, collectivity is closely associated with a density of levels ($\sim m^*$) consistent with an effective mass $m^* = m_\omega m_k/m \approx m$. This is achieved by coupling the two-quasiparticle QRPA SLy4 solutions to 4qp doorway states made out of a 2qp uncorrelated component and an empirically tuned QRPA collective mode [25] (see Fig. 2 of [7], cf. also [26]), an example of the fact that in a consistent PVC renormalised description of the nuclear structure, one has to treat (dress), on equal footing, all degrees of freedom (i.e. single-particle and collective modes). In this way, not only self-energy but also vertex corrections are consistently included (sum rules conserving processes), and thus the "bare" QRPA mode is properly clothed, bringing theory in overall agreement with experiment (see Table 1, second and third lines; for details cf. [27] as well as [7]).

To test how robust the results displayed in Fig. 1 are, we have recalculated $\tilde{\Delta}_\nu$ as a function of the three parameters $\{\ m_k,\ v_p^{bare},\ \beta_J(J^\pi)\ \}$ [28][29][25]. The results ($|\Delta_{h11/2} - \Delta^{exp}|$) associated with the lowest quasiparticle state $h_{11/2}$ are displayed in Figs. 2(a),(b) and (c). They provide evidence of the fact that a description based on the renormalisation of single-particle states and collective modes through PVC leads to a well funnelled nuclear structure landscape [30], displaying a global minimum for values of the set of parameters $\{\ \}$ close to the empirical values: effective mass $m_k \approx 0.7m$, bare pairing interaction strength v_p^{bare} consistent with $v_{14}(^1S_0)(G_0 \approx 0.22$ MeV, see [29]) and quadrupole deformation parameter $(\beta_2)_0 \approx (\beta_2)_{exp} \approx 0.13$.

Similar conclusions can be drawn from the study of the dependence on v_p^{bare} and β_2 of the

quasiparticle spectrum associated with the valence orbitals ($h_{11/2}, d_{3/2}, s_{1/2}, g_{7/2}$ and $d_{5/2}$), of the splitting of the multiplet of states $(h_{11/2} \otimes 2^+)_{15/2^- - 7/2^-}$ and of the $\gamma-$decay spectrum following Coulomb excitation, as can be seen from Figs. 2(d)-(f), Figs.2(g)-(h) and Fig.3, respectively.

Because of the PVC mechanism, the different valence quasiparticle states undergo renormalization and fragmentation, phenomena which can be specifically probed with one-particle transfer reactions. In Fig. 4(a) we display the absolute differential cross sections associated with the reaction $^{120}Sn(d,p)^{121}Sn(lj)$, calculated making use of the spectroscopic amplitudes associated with the strongest populated fragments of the valence orbitals $h_{11/2}, d_{3/2}, s_{1/2}$ and $d_{5/2}$ and of global optical parameters, in comparison with the experimental data [33]. Theory provides an overall, quantitative , account of the experimental findings. To be noted that the agreement found between the summed absolute differential cross sections associated with the almost degenerate state $3/2^+$ and $11/2^-$ (experimentally non resolvable [33], while theoretically separated by 100 keV), results from a subtle incoherent combination of the $l = 2, d\sigma_{1n}/d\Omega$ peak at $\theta_{CM} \approx 20^0$ and of that of the $l = 4$ one at $\theta_{CM} = 47^0$.

In discussing the ^{120}Sn$(p,d)^{119}$Sn reaction we concentrate on the $d_{5/2}$ orbital, the most theoretically challenging of all of the valence single-particle strength functions. This is because this state, being further away from the Fermi energy ($\epsilon_{d_{5/2}} = -11.3$ MeV, $\epsilon_F \approx -8$MeV) than the other four valence orbitals (see Table 2), is embedded in a denser set of doorway states (of type $s_{1/2} \otimes 2^+, d_{3/2} \otimes 2^+, g_{7/2} \otimes 2^+, h_{11/2} \otimes 3^-$, etc.), as compared to the other ones. Consequently, it can undergo accidental degeneracy and thus conspicuous fragmentation. As seen from Table 3, although the calculated summed cross sections ($\sigma =$ 6.15 mb) agree, within experimental errors, with observation (7.93 ± 2 mb), theory predicts an essentially uniform fragmentation of the strength over an energy interval of ≈ 760 keV, while the data [32] is consistent with a concentration of the strength at an energy close to that of the lowest theoretical $5/2^+$ level (1090 keV).

In keeping with the above scenario we have shifted the bare single-particle energy $\epsilon_{d_{5/2}}$ by 600 keV ((-11.3 + 0.6) MeV= - 10.7 MeV), amounting to a 6% change in the $k-$mass (i.e. from $0.7m$ to $0.74m$, Table 2), and recalculated all the quantities discussed above. Making use of the corresponding nuclear structure results and of global optical parameters, the absolute differential cross sections associated with the $5/2^+$ states populated in the reaction $^{120}Sn(p,d)^{119}Sn$ and lying below 2 MeV have been calculated. They are displayed

in Fig. 4(b) in comparison with the experimental data. Theory provides now a quantitative account of the experimental findings. In particular, of the fact that the strength function is dominated by a single peak. With the 600 keV shift, it is predicted at an energy of 1050 keV carrying 4.4 mb and it is observed at 1090 keV with a cross section of 5.35 $\pm$1.3 mb. The resulting overall agreement between theory and experiment is further confirmed by Fig. 4(c) where the absolute value of the one-particle transfer strength function associated with the population of $5/2^+$ states predicted by the calculation is compared with experiment. As observed in Fig. 4(d), also this two-dimensional projection of the multidimensional nuclear structure landscape is funnelled, testifying to the physical robustness of the findings.

An alternative approach to the one discussed above which leads to almost identical findings regarding the $d_{5/2}$ fragmentation, can be obtained by treating the energy of the five valence orbitals as parameters to be optimized selfconsistently within the framework of the full NG calculations, so as to best reproduce the quasiparticle spectrum (Opt. Table 2). The results can be expressed in terms of a state-dependent $k-$mass $\langle (m_k)_\nu/m \rangle \approx 0.74 \pm \sigma$, with $\sigma = 0.07$.

Making again use of the effective occupation numbers resulting from the solution of the NG equation, the two-nucleon spectroscopic amplitudes of the reactions $^{120}Sn(p,t)^{118}Sn(gs)$ and $^{122}Sn(p,t)^{120}Sn(gs)$ have been calculated. With the help of these quantities and of global optical parameters, the absolute differential cross sections have been calculated in second-order DWBA taking into account successive and simultaneous transfer, properly corrected from non-orthogonality contributions [34]. They are displayed in Figs 1(b) and 1(c) in comparison with the experimental findings [35, 36]. Theory reproduces the absolute differential cross sections associated with the ground state transitions within experimental errors. The calculations have been repeated for different values of the strength of the PVC associated with the most important collective vibrational mode, namely the lowest 2^+ as well as for different strengths of the bare pairing interaction. While the dependence of $\sigma_{2n}(p,t)$ is very weak with β_2 (not shown), it is conspicuous with v_p^{bare}. An example of such dependence is displayed in the inset to Fig. 1(a). Again, this two-dimensional section of the nuclear structure landscape is of a well funnelled character. Within this context, it is noted that a measure of the reliability with which theory can describe the nuclear structure is provided by the relative dimensionless standard deviations σ_{rel} (equal to e.g. $\sigma(E_{qp})/\langle E_{qp} \rangle$ in the case of the quasiparticle spectrum) associated with each of the different observables, and taken

at the minimum of the nuclear structure landscape, as shown in Table 4.

We conclude that a theoretical description of nuclear structure based on single-particle (mean field with $m_k \approx 0.7m$) and collective motion (QRPA) and on their interweaving controlled by the particle-vibration coupling mechanism and leading to renormalization of both types of nuclear excitations through mass (self-energy) and screening (vertex) corrections and induced pairing, can provide an overall quantitative account of the nuclear structure representative of a mass zone (group of nuclei displaying homogeneous properties like e.g. sphericity and superfluidity, likely circumscribed by phase transition domains). Allowing for a weak state dependence of the k–mass, determined by optimising the energy of the valence single-particle orbitals to reproduce the quasiparticle spectrum, the theoretical description of the nuclear structure probed in terms of direct reaction absolute differential cross sections and based on renormalized single–particle and collective degrees of freedom, becomes accurate within a 10% error level. The PVC mechanism is found to play a central role in achieving this result. Within this context, we note that pairing in typical superfluid nuclei lying along the stability valley like ^{118,119,120,121,122}Sn has a dual origin, in which v_p^{bare} and v_p^{ind} contribute essentially equally to the pairing gap. The above considerations and protocols are not only transferable to the remaining superfluid Sn-isotopes (not considered explicitely in the present case), but also applicable to the quantitative description of other spherical, superfluid nuclear mass zones.

I. ACKNOWLEDGMENTS

This work have been supported by the Academy of Finland and University of Jyväaskylä within the FIDIPRO program and by the Helmholtz Association through the Nuclear Astrophysics Virtual Institute (VH-VI-417) and the Helmholtz International Center for FAIR within the framework of the LOEWE program launched by the state of Hesse.

[1] A. Bohr and B.R. Mottelson, *Nuclear structure*, Vol. II, (Benjamin, New York, 1975)

[2] A. Bohr, *Rotational motion in nuclei*, Le Prix Nobel en 1975, Norstedts Tryckeri, Stockholm (1976), 56

[3] B.R. Mottelson, *Elementary modes of excitation in nuclei*, Le Prix Nobel en 1975, Norstedts Tryckeri, Stockholm (1976), 80

[4] *Proceedings of the International Nuclear Physics Conference*, Florence 2013, S. Lunardi et al. eds., EPJ Web Conf. **66** (2014)

[5] *50 Years of Nuclear BCS*, R.A. Broglia and V. Zelevinsky eds., World Scientific, Singapore (2013)

[6] D. Tarpanov, J. Dobaczwewski, J. Toivanen and B.G. Carlsson, Phys. Rev. Lett. **113**, 252501 (2014)

[7] F. Barranco, R.A. Broglia, G. Colò, G. Gori, E. Vigezzi and P.F. Bortignon, Eur. Phys. J. A**21**, 57 (2004)

[8] A.V. Avdeenkov and S.P. Kamerdzhiev, Phys. At. Nucl. **62** (1999) 563

[9] S.P. Kamerdzhiev, A.V. Avdeenkov and D.A. Voitenkov, Phys At. Nucl. **74** (2011) 1478

[10] E. Litvinova and A.V. Afanasjev, Phys. Rev. C **84** (2011) 014305

[11] E. Litvinova, Phys. Rev. **C 85**, 021303 (2012)

[12] P. Ring and E. Litvinova, Phys. At. Nucl. **72** (2009) 1285

[13] G. Colò, H. Sagawa and P.F. Bortignon, Phys. Rev. C **82** (2010) 064307

[14] K. Mizuyama, G. Coló, E. Vigezzi, Phys. Rev. **C 86** (2012) 034318

[15] N.V. Gnezdilov, N. Borzov, E.E. Saperstein, S.V. Tolokonnikov, Phys. Rev. C **89** (2014) 034304

[16] A. Idini, F. Barranco and E. Vigezzi, Phys. Rev. C **85**, 014331 (2012)

[17] A. Idini, *Renormalization effects in nuclei*, Ph.D. Thesis, University of Milan (2013), http://air.unimi.it/2434/216315

[18] J. Schrieffer, *Superconductivity* (Benjamin, New York, 1964)

[19] D. Van Neck, M. Waroquier, V. Van der Sluys and J. Ryckebusch, Nucl. Phys. A **563** (1993) 1

[20] V. Somà, C. Barbieri and T. Duguet, Phys. Rev. C **89**, 024323 (2014)

[21] P.F. Bortignon, R.A. Broglia and C.H. Dasso, Nucl. Phys. A **398**, 221 (1983)

[22] H.-J. Schulze, J. Cugnon, A. Lejeune, M. Baldo, and U. Lombardo, Phys. Lett. B 375, 1 (1996).

[23] H. Heiselberg, C.J. Pethick, H. Smith and L. Viverit , Phys. Rev. Lett. 85 (1000) 2418

[24] J. Terasaki, J. Engel and G.F. Bertsch, Phys. Rev. C78, 044311 (2008)

[25] This mode, used also in the calculation of the different quantities as a function of β_2, is determined as the QRPA solution of a separable multipole–multipole interaction with empirical single-particle levels, adjusting the strength to obtain the desired properties. One avoids in this way the difficulties associated with the zero–range character (ultraviolet divergencies) and finite size instabilities of most Skyrme forces (cf. [37, 38] and refs. therein) . This procedure is what is called empirical renormalization in the text.

[26] G. Bertsch, P.F. Bortignon and R.A. Broglia, Rev. Mod. Phys. 55 , 287 (1983)

[27] F. Barranco et al, to be published

[28] In the calculation of the pairing gap $\Delta_{h_{11/2}}$ as a function of m_k, the full NG solution was worked out for the Skyrme interactions Ska (m_k/m= 0.61), SAMi (0.67), SLy4 (0.70), SGII (0.79), SkM* (0.79), SkS1 (0.86) and SkP (1.0) and the corresponding quantity extracted (continuous curve in Fig. 2(a)).

[29] In carrying out the calculations reported in Figs. 2(b) and 2(f), namely the pairing gap $\Delta_{h11/2}$ and the deviation of the quasiparticle spectrum from experiment as a function of the strength of the bare $NN-$pairing force $v_{14}(^1S_0)$, the average value of the matrix elements of this interaction has been parametrised in terms of a monopole-monopole pairing force with constant matrix elements G. The reference value $G_0(\approx 0.22$ MeV) has been determined so as to reproduce, in average, the $v_{14}(^1S_0)$ value of Δ_{j_ν} of the valence states.

[30] H. Frauenfelder, S.G. Sligar and P.G. Wolynes, Science **254** (1991) 1598

[31] P.H. Stelson, W.T. Milner, F.K. McGowan, R.L. Robinson and S. Raman, Nucl. Phys. **190** (1972) 197

[32] S. Dickey, J. Kraushaar, R.Ristinen and M. Rumore, Nucl. Phys. A **377**, 137 (1982)

[33] M.J. Bechara and O. Dietzch, Phys. Rev. C**12**, 90 (1975)

[34] G. Potel, A. Idini, F. Barranco, E. Vigezzi and R.A. Broglia, Rep. Prog. Phys. **76**, 106301 (2013)

[35] P. Guazzoni et al., Phys. Rev. C**78**, 064608 (2008)

[36] P. Guazzoni et al., Phys. Rev. C**60**, 054603 (1999)

[37] V. Hellemans, Phys. Rev. C**88**, 064323 (2013)

[38] D. Tarpanov, A. Pastore, D. Davesne, J. Navarro, Spurious finite–size instabilities in nuclear energy density functionals: spin channel, to be published

	$\hbar\omega_{2+}$ (MeV)	B(E2 $\uparrow$) (e^2 fm^4)	β_2
QRPA (SLy4)	1.5	890	0.06
QRPA + REN	0.9	2150	0.14
Exp.	1.2	2030	0.13

TABLE I. Energy, reduced E2 transition strength and corresponding deformation parameter β_2 associated with the low-lying 2^+ state of ^{120}Sn, calculated according to QRPA and empirically renormalized QRPA as explained in the text, are compared to the experimental values [31].

Orbital	ε_ν (MeV)		$(m_k)_\nu/m$
	SLy4	Opt.	
$d_{5/2}$	-11.3	-10.7	0.74
$g_{7/2}$	-10.1	-10.5	0.67
$s_{1/2}$	-9.0	-7.9	0.80
$d_{3/2}$	-8.5	-7.1	0.83
$h_{11/2}$	-7.1	-7.45	0.67
			0.74 ($\sigma = 0.07$)

TABLE II. Energy of the valence orbitals associated with SLy4 ($m_k = 0.7m$) and those obtained by optimizing (Opt.) the NG quasiparticle spectrum to the data. In the last column the results labeled Opt. are parametrized in terms of an effective, state dependent k-mass.

	Exp.			Th.	
ϵ_i (keV)	σ (mb)	$d\sigma/d\Omega$ (mb/sr)	ϵ_i (keV)	σ (mb)	$d\sigma/d\Omega$ (mb/sr)
921	0.63	0.75	1150	1.80	2.3
1090	5.35	7.0	1290	1.20	1.7
1354	1.66	2.3	1710	0.25	0.32
1562	0.13	0.16	1910	2.90	4.0
1730	0.16	0.18			
	7.93 ± 2	10.39		6.15	8.32

TABLE III. The most prominent experimental (theoretical) fragments of the $d_{5/2}$ single-particle state populated in the ^{120}Sn(p,d) ^{119}Sn ($5/2^+$) reaction. The energies are listed in the first (fourth) column, while the absolute cross sections are given in the second (fifth), integrated within the range $2^0 < \theta_{CM} < 55^0$, and third (sixth), peak cross section, $(\theta_{CM})_{max} \approx 17^0$. The data are from [32].

Observables	SLy4	$d_{5/2}$ shifted	Opt. levels
Δ	10 (0.7%)	10 (0.7 %)	50 (3.5 %)
E_{qp}	190 (19%)	160 (16%)	45 (4.5 %)
Mult. splitt.	50 (7%)	70 (10%)	59 (8.4 %)
$d_{5/2}$ strength (centr.)	200 (20%)	40 (4%)	40 (4%)
$d_{5/2}$ strength (width)	160 (20%)	75 (9.3%)	8 (1%)
$B(E2)$	1.4 (14%)	1.34 (13%)	1.43 (14%)
$\sigma_{2n}(p,t)$	0.6 (3%)	0.6 (3%)	0.6 (3%)

TABLE IV. Mean square deviation σ between the experimental data and the theoretical values taken at the minimum of the corresponding functions displayed in Figs. 1(a) (inset),2(c,e,h),3(b) and 4(d) in keV for the pairing gap, quasiparticle energies, multiplet splitting, centroid and width of the $5/2^+$ low-lying single-particle strength distribution. In single-particle units B_{sp} for the γ-decay (B(E2) transition probabilities) and in mb for $\sigma_{2n}(p,t)$. In brackets the ratio σ/L, called σ_{rel} in the text, between σ and the experimental range L of the corresponding quantities: 1.4 MeV (Δ), 1 MeV (E_{qp}), 700 keV (mult. splitting), 1 MeV ($d_{5/2}$ centroid), 809 keV (=1730- 921) keV ($d_{5/2}$ width), 10 B_{sp} (B(E2)), 2250 mb ($\sigma_{2n}(p,t)$), is given.

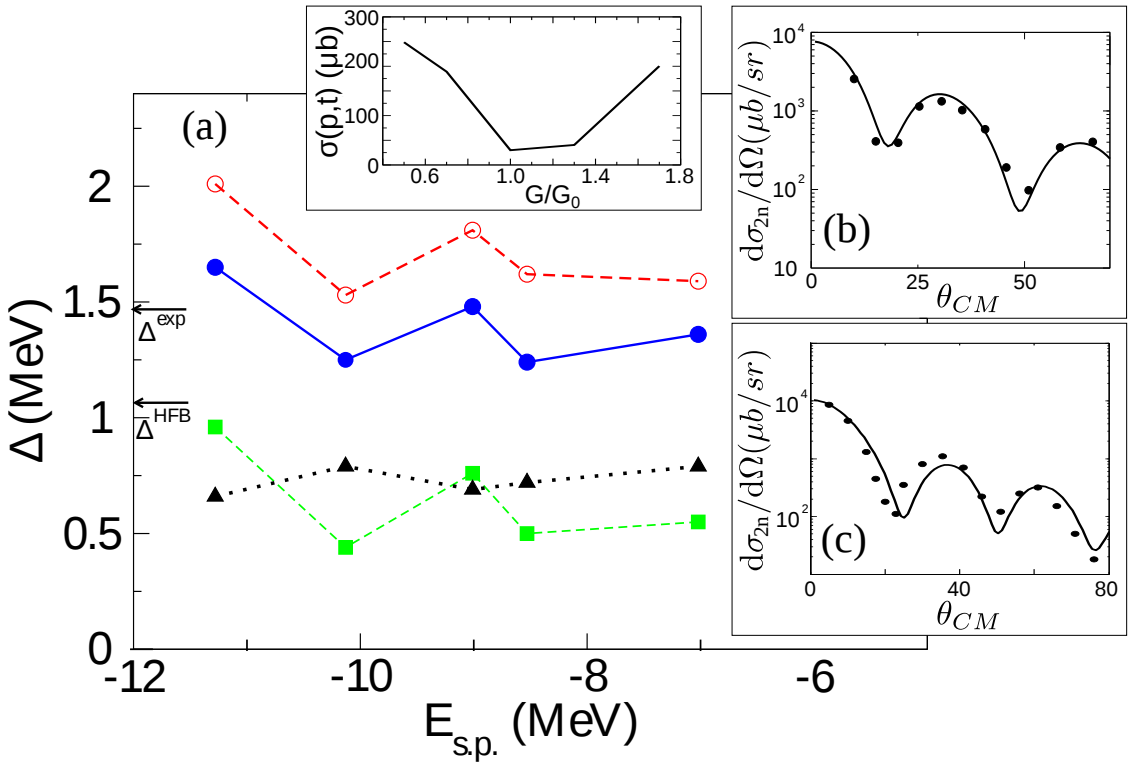

FIG. 1. **(a)** State-dependent pairing gaps for the five valence orbitals of ^{120}Sn (see Table II, second column). The value of Δ associated with the HFB solution of $v_{14}(^1S_0)$) is indicated by an arrow labeled Δ^{HFB}. The pairing gaps calculated making use of the empirically renormalised density modes are shown in terms of open circles joined by a dashed line, while the corresponding results obtained including also spin modes, and thus corresponding to $\tilde{\Delta}_\nu$ are shown by the solid dots joined by a continuous curve. The contributions $\tilde{\Delta}_\nu^{bare}$ and $\tilde{\Delta}_\nu^{ind}$ are displayed in terms of solid triangles and solid squares joined by dotted and by dashed lines respectively. **(b,c)** Calculated two-particle transfer absolute differential cross sections associated with the reactions ^{120}Sn(p,t)^{118}Sn (gs) and $^{122}Sn(p,t)^{120}Sn(gs)$ (continuous curves) in comparison with experimental data (solid dots) [35, 36]. In the inset of (a), the absolute value of the deviation of the integrated theoretical absolute cross section from the experimental value in the case of the second reaction is given as a function of the strength of the bare pairing interaction (cf. [29]).

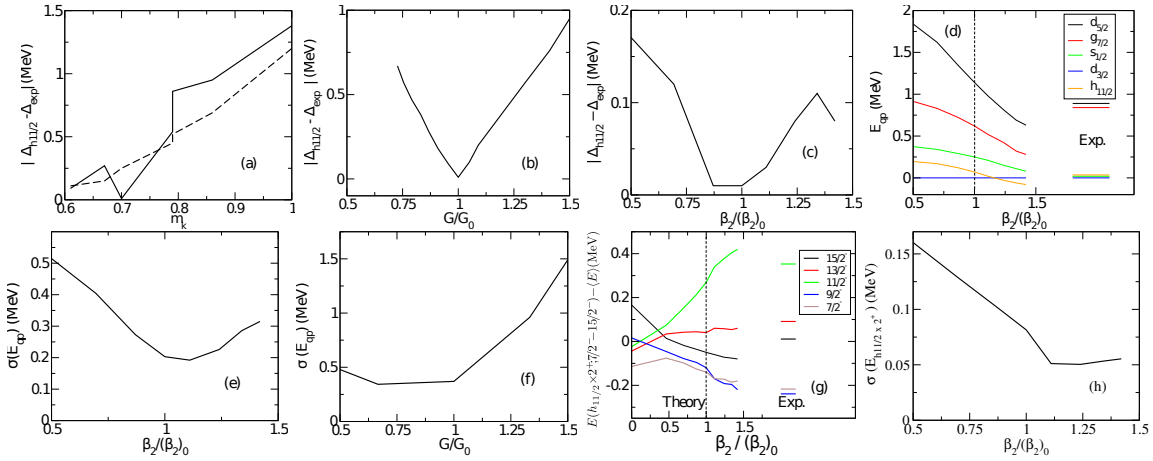

FIG. 2. Absolute value of the difference between the experimental pairing gap and the theoretical value of $\Delta_{h_{11/2}}$ (see Eq.(1)), calculated: **(a)** as a function of the effective mass m_k associated with different Skyrme forces (solid curve) [28], the dashed curve displaying the gap obtained using the fixed set of valence levels $\epsilon_\nu(Opt.)$ (Table II); **(b)** as a function of the ratio G/G_0 [29]; **(c)** as a function of the ratio $\beta_2/(\beta_2)_0$ associated with the lowest quadruple mode of ^{120}Sn [25]. **(d)** (color online) The lowest quasiparticle energy values obtained from the full calculation as explained in the text referred to the energy of the $3/2^+$ state, in comparison with the experimental data. **(e)** Mean square deviation between the experimental and theoretical levels shown in (d). **(f)** Mean square deviation between the experimental and theoretical energies of the five valence levels, as a function of the ratio G/G_0. **(g)** (color online) The experimental energies of the members of the $h_{11/2} \otimes 2^+$ multiplet are compared with the theoretical values, calculated as a function of the ratio $\beta_2/(\beta_2)_0$. **(h)** Mean square deviation between the experimental and theoretical energies of the members of the $h_{11/2} \otimes 2^+$ multiplet shown in (g).

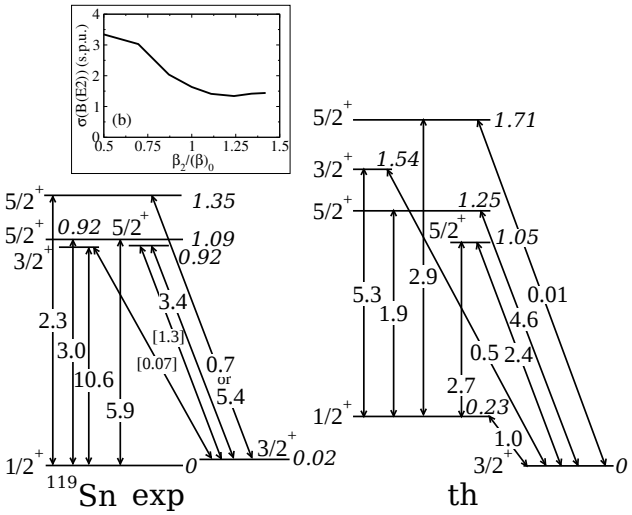

FIG. 3. Experimental B(E2) values [31] in units of B_{sp}, of the quadrupole $\gamma-$ decay following $^{119}Sn(\alpha,\alpha')^{119}Sn^*$ Coulomb excitation, connecting the low-lying states of ^{119}Sn (left). Also given are the theoretical values calculated making use of the results of the full renormalised calculation as explained in the text (right). The energies are in MeV. Mean square deviation between the experimental transition strengths associated with E2 decay from the $5/2^+$ levels, and the theoretical values calculated as a function of the β_2 parameter is given in the inset (upper left).

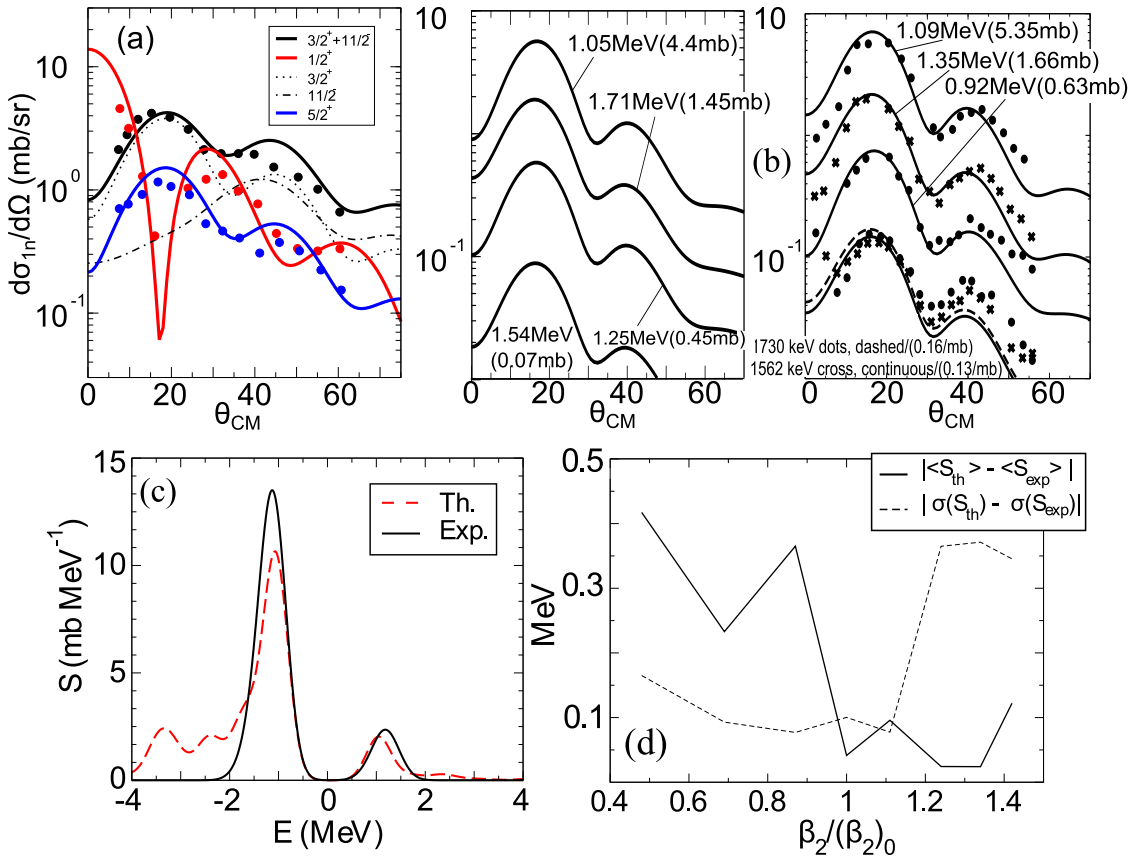

FIG. 4. **(a)** (color online) Absolute finite range, full recoil DWBA theoretical differential cross sections associated with the low–lying fragments of the $h_{11/2}, d_{3/2}, s_{1/2}$ and $d_{5/2}$ valence states most strongly populated in the reaction ^{120}Sn(d,p)^{121}Sn, calculated with the help of state of the art optical potentials and v_{np} interaction (I.J. Thompson, private communication), making use of NG structure input, in comparison with the experimental data [33]. It is of notice that the $d_{5/2}$ single-particle orbit in the SLy4 mean field potential has been shifted towards ϵ_F by 0.6 MeV (see text). **(b)** ^{120}Sn(p,d)^{119}Sn $(5/2^+)$ absolute experimental differential cross sections [32], together with the DWBA fit used in the analysis of the data (right panel) in comparison with the DWBA calculations (left panel) carried out as mentioned in (a) . **(c)** Comparison of the calculated strength function $S_{5/2}(\sigma(^{120}Sn(p,d)^{119}Sn(5/2^+)+\sigma(^{120}Sn(d,p)^{121}Sn(5/2^+))/E$ with experimental data derived from one-neutron transfer reactions [32, 33]. The peaks have been folded together with a Gaussian function of variance 0.25 MeV. **(d)** The difference between the centroid (width) of the experimental and of the calculated $d_{5/2}$ strength $S_{5/2}$ is shown as a function of the ratio $\beta_2/(\beta_2)_0$ in terms of the solid (dashed) curve.